

# Comparison of Measured and Modeled Nocturnal Clear Sky Longwave Downward Radiation at Payerne, Switzerland

Wacker S.<sup>a</sup>, Gröbner J.<sup>a</sup>, Emde C.<sup>b</sup>, Vuilleumier L.<sup>c</sup>, Mayer B.<sup>b</sup>, Rozanov E.<sup>a</sup>.

<sup>a</sup>*Physikalisch-Meteorologisches Observatorium Davos/World Radiation Center (PMOD/WRC), Davos, Switzerland*

<sup>b</sup>*Deutsches Zentrum für Luft- und Raumfahrt (DLR), Institut für Physik der Atmosphäre, Oberpfaffenhofen, Germany*

<sup>c</sup>*Meteo Swiss, Payerne, Switzerland*

**Abstract.** In this study, a comparison of measured and modeled nocturnal clear sky Longwave Downward Radiation (LDR) in Payerne, Switzerland, was performed. The Radiative Transfer Models (RTM) MODTRAN and libRadtran were applied to compute LDR irradiances. Absorption coefficients for libRadtran calculations were generated using the line-by-line model ARTS and the band model LOWTRAN. 39 clear nights were chosen to calculate LDR and to compare with broadband LDR measurements and LDR measurements taken in the wavelength range 8 to 14  $\mu\text{m}$ . To run the models, two different types of vertical pressure, temperature and humidity profiles were implemented: (a) radiosonde profiles normalized to 2 meter ground values of pressure, temperature and humidity and scaled to the total Integrated Water Vapor (IWV) content; (b) seasonal standard profiles of the McClatchey midlatitude atmosphere normalized to ground measurements and scaled to the total IWV content. In the broadband range, MODTRAN revealed mean differences (measured minus calculated LDR) of  $-1.2 \text{ Wm}^{-2} \pm 2.5 \text{ Wm}^{-2}$  and  $+7.7 \text{ Wm}^{-2} \pm 5.2 \text{ Wm}^{-2}$  for profile (a) and (b) respectively. In the wavelength range 8 to 14  $\mu\text{m}$ , mean differences were  $-1.4 \text{ Wm}^{-2} \pm 2.0 \text{ Wm}^{-2}$  and  $+2.1 \text{ Wm}^{-2} \pm 3.7 \text{ Wm}^{-2}$ . LOWTRAN revealed mean biases of  $+6.0 \text{ Wm}^{-2} \pm 2.9 \text{ Wm}^{-2}$  and  $+14.2 \text{ Wm}^{-2} \pm 5.6 \text{ Wm}^{-2}$  in the broadband range. In the wavelength range 8 to 14  $\mu\text{m}$ , the biases were  $+4.1 \text{ Wm}^{-2} \pm 2.4 \text{ Wm}^{-2}$  and  $+7.4 \text{ Wm}^{-2} \pm 4.1 \text{ Wm}^{-2}$  for profile (a) and (b) respectively. Line-by-line calculations using ARTS were only performed with profile (a) in the wavelength range 8 to 14  $\mu\text{m}$ . Results showed a mean difference of  $-0.7 \text{ Wm}^{-2} \pm 2.0 \text{ Wm}^{-2}$  between measurements and computations.

**Keywords:** LDR, pyrgeometer, atmospheric window, ARTS, MODTRAN, libRadtran, LOWTRAN.

**PACS:** 92.60 Aa

## 1. INTRODUCTION

The surface radiation budget plays a fundamental role in the climate system of the earth. It determines the exchange of energy between the surface and the atmosphere and therefore controls the atmospheric and oceanic circulations. Longwave Downward Radiation (LDR), emitted by the sky, is thereby a key component in the surface radiation budget. Hence, an accurate knowledge of LDR is required to understand and predict future changes in the surface radiation budget.

This investigation was carried out in the frame of the Longwave Infrared Radiative forcing trend Assimilation over Switzerland (LIRAS) – project. The LIRAS project aims to investigate LDR in Switzerland and to produce trend estimates of LDR using observation data, statistical tools and radiative transfer models (RTM). Particular attention in the project is paid to the wavelength range from about 8 to 14  $\mu\text{m}$ , where the cloud free atmosphere is relatively transparent to longwave radiation. This wavelength region is referred to as the atmospheric window. Most of the changes in LDR occur in this wavelength range. In order to measure the evolution of LDR in the atmospheric window, modified CGR3 pyrgeometers, sensitive only in the atmospheric window, were acquired.

This study investigated the performance of three absorption models with different spectral resolution. The band models LOWTRAN and MODTRAN were applied over the broadband range and in the atmospheric window under nocturnal clear sky conditions compared to measurements in the corresponding wavelength range. Furthermore, pyrgeometer measurements in the atmospheric window were compared to line-by-line results accomplished with the line-by-line tool ARTS.

## 2. OBSERVATIONAL DATA

### 2.1 Instruments and LDR Measurements

LDR measurements in Payerne/Switzerland (Lat. 46.81° N, Long. 6.94° E, Alt. 490 masl) were obtained in one minute time intervals from a broadband Kipp & Zonen CG4 pyrgeometer and a modified Kipp & Zonen CGR3 pyrgeometer sensitive only in the atmospheric window. Pyrgeometers are commonly used instruments to measure longwave radiation. The longwave radiative energy is thereby transformed to an output voltage by a black painted thermophile sensor. The output voltage of the thermophile arises from the absorption and emittance of thermal radiation through a silicon dome. The dome rejects radiation from wavelengths shorter than about 4  $\mu\text{m}$ . We equipped a conventional broadband CGR3 pyrgeometer with an additional Germanium band pass filter transmitting only longwave radiation from about 8 to 14  $\mu\text{m}$ . To obtain LDR from such a modified CGR3 pyrgeometer, the radiation balance at the sensor surface has to be solved considering the spectral wavelength range from 8 to 14  $\mu\text{m}$  [1]. This results in:

$$LDR = \frac{U_{rec}}{C} (1 + k_1 \sigma T_B^3) + k_2 \sigma \int_{8\mu\text{m}}^{14\mu\text{m}} L_\lambda(T_B) d\lambda. \quad (1)$$

with  $U_{rec}$  the output voltage of the thermophile,  $C$  the sensitivity factor of the pyrgeometer,  $k_1$  and  $k_2$  as correction factors describing absorptance, transmittance, reflectance of the silicon dome and emittance of the thermophile sensor,  $\sigma$  the Stefan-Boltzmann constant,  $T_B$  the body temperature of the pyrgeometer measured by an internal thermistor and  $L_\lambda$  the Planck function.  $k_1$ , and  $k_2$  are instrument parameters which are determined individually for each pyrgeometer. The sensitivity  $C$  of the CGR3 pyrgeometer is determined in the reference blackbody of PMOD, while for the CG4 pyrgeometer  $C$  is determined relative to the World Infrared Standard Group (WISG) of pyrgeometers during an outdoor comparison [2]. The use of different calibration procedures for the CGR3 and CG4 pyrgeometers is due to their different spectral sensitivity ranges which preclude a laboratory calibration of a broadband pyrgeometer using a blackbody cavity [3]. The modified CGR3 pyrgeometers were calibrated several times in spring 2007 and winter 2007/2008. The uncertainties of the measured longwave irradiances are estimated to about  $\pm 2 \text{ Wm}^{-2}$  and  $\pm 1 \text{ Wm}^{-2}$  for the CG4 and CGR3 pyrgeometers respectively.

### 2.2 ADDITIONAL OBSERVATIONAL DATA

Balloon SRS 400 radiosondes measuring pressure, temperature and humidity are accomplished twice a day at Payerne. The sondes are launched around 11 and 23 UTC. Measured pressure and temperature profiles extend from ground to approximately 35 km, whereas the measured humidity profile ends at about 12 km masl. The vertical resolution in the troposphere is approximately 15 meters. However, there are some difficulties encountered with the hygistor concerning limited sampling below temperatures of -30 °C leading to slightly overestimated values [4]. Hence, the total integrated water vapor (IWV) content, derived from GPS measurements was applied in the RTM to scale the radiosonde humidity profiles. The GPS signal is provided by the Automated GPS Network of Switzerland (AGNES) – station at Payerne. IWV values derived from GPS measurements are available from the Studies in Atmospheric Radiative Transfer and Water Vapor Effects (STARTWAVE) database of the University Bern [5].

CO<sub>2</sub> measurements were obtained from the regional Global Atmospheric Watch (GAW) station Schauinsland located in Southern Germany. The last available value from December 2006 was thereby interpolated using a simplified yearly cycle of 10 ppm CO<sub>2</sub> and a trend of + 2 ppm(yr)<sup>-1</sup> [6]. The vertical total ozone column was provided by the Aura spacecraft.

### 2.3 Clear Sky Detection

We applied the Automatic Partial Cloud Amount Detection Algorithm (APCADA) to identify clear sky situations [7]. APCADA uses LDR, humidity and temperature measurements at 2 meters above ground, standard deviation of LDR during the last hour and a set of empirical rules to compute cloud cover in octas. We selected situations with an estimated cloud amount not exceeding one octa for  $\pm 1.5$  hours around 23 UTC when the radiosonde is launched. A total of 39 cases in the period 2007 to 2008 were chosen representing all four seasons.

### 3. MODELS AND INPUT DATA

The model calculations were performed with the RTM libRadtran [8] and MODTRAN [9]. libRadtran calculations have been performed with two different absorption models: Highly resolved absorption coefficients were calculated using the line-by-line model ARTS [10] and for faster computation the relatively low resolution band model LOWTRAN [11] as adapted from the SBDART code [12] was used. The calculations were done in the spectral range from 2 to 300  $\mu\text{m}$ . ARTS line-by-line calculations were based on the HITRAN 2004 database, whereas MODTRAN and LOWTRAN apply an approximation of the absorption lines, a so called band parameterization. The parameterization requires considerably less computational time than line-by-line calculations, but is less accurate. The LOWTRAN band model has a resolution of 20  $\text{cm}^{-1}$ . MODTRAN, however, uses an improved parameter model with a resolution of 1  $\text{cm}^{-1}$ .

Two different types of vertical profiles were used in the models: In profile type (a) vertical profiles of pressure, temperature and humidity obtained from radiosondes were implemented into the models. Above the sonde profiles, missing values were filled up to 100 km masl with data from the McClatchey midlatitude atmospheres. Profile type (b) was deduced from pressure, temperature and humidity profiles of the McClatchey midlatitude summer (May – September) or McClatchey midlatitude winter atmosphere (October – April), i.e. no radiosonde data were used. Profile (b) was used in order to infer the performance of RTM for sites where no radiosonde data are available. All pressure, temperature and humidity profiles were normalized to 2 meter ground measurements from the weather station at about 23 UTC (sonde launch). Humidity profiles were scaled to the total IWV content as noted above.

The default profiles of the greenhouse gases  $\text{CO}_2$  and  $\text{O}_3$  were scaled to the corresponding observations mentioned above. In order to keep consistency among the models, aerosols were not included. Some MODTRAN runs accomplished with the rural aerosol type, including a surface meteorological range of 34 km, revealed an increase in LDR of about 1  $\text{Wm}^{-2}$  relative to the LDR irradiance.

### 4. RESULTS

In order to compare measurements and computations, the LDR measurements were averaged over 30 minutes to account for the radiosonde ascent. Line-by-line calculations were only performed for profile (a) and for the atmospheric window.

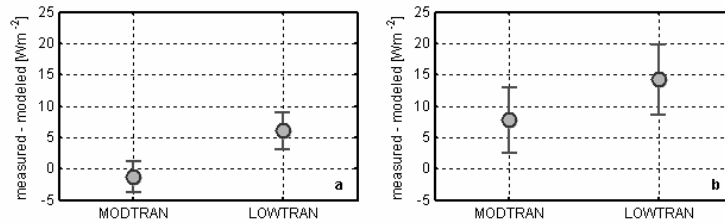


**FIGURE 1.** Mean difference and its standard deviation of measured and modeled broadband LDR for profile (a) (normalized radiosonde profile scaled to IWV) (a) and for profile (b) (normalized standard profile of McClatchey midlatitude atmosphere scaled to IWV) (b).

Figure 1 represents the results of the mean bias and its standard deviation of measured and modeled broadband LDR for the two profiles. MODTRAN revealed a mean difference of  $-1.2 \text{ Wm}^{-2} \pm 2.5 \text{ Wm}^{-2}$  for profile (a) and  $+7.7 \text{ Wm}^{-2} \pm 5.2 \text{ Wm}^{-2}$  applying profile (b). The mean bias of LOWTRAN of  $+6.0 \text{ Wm}^{-2} \pm 2.9 \text{ Wm}^{-2}$  and  $+14.2 \text{ Wm}^{-2} \pm 5.6 \text{ Wm}^{-2}$  for profile (a) and (b) respectively was due to the lower resolved band parameter model.

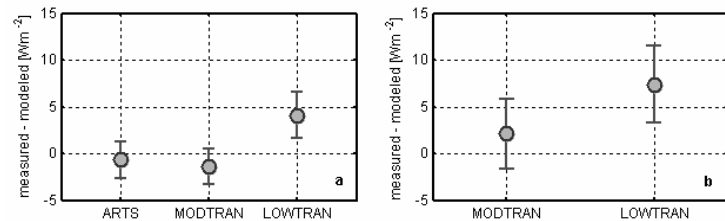


**FIGURE 2.** Mean difference and its standard deviation of measured and modeled LDR in the atmospheric window for profile (a) (normalized radiosonde profile scaled to IWV) (a) and for profile (b) (normalized standard profile of McClatchey midlatitude atmosphere scaled to IWV) (b). ARTS results were only computed for profile (a).

Figure 2 summarizes the results for the atmospheric window. As for the broadband range, the MODTRAN calculations agreed with a mean difference of  $-1.4 \text{ Wm}^{-2} \pm 2.0 \text{ Wm}^{-2}$  very well with the measurements for profile (a). These results were confirmed by the line-by-line model ARTS revealing a mean bias of  $-0.7 \text{ Wm}^{-2} \pm 2.0 \text{ Wm}^{-2}$ . In fact, even for profile (b) the agreement of  $+2.1 \text{ Wm}^{-2} \pm 3.7 \text{ Wm}^{-2}$  was, in contrast to the broadband range, almost as good as for profile (a). For LOWTRAN, mean differences of  $+4.1 \text{ Wm}^{-2} \pm 2.4 \text{ Wm}^{-2}$  and  $+7.4 \text{ Wm}^{-2} \pm 4.1 \text{ Wm}^{-2}$  for profile (a) and (b) respectively, were considerably higher compared to MODTRAN, as in the broadband range.

## 5. CONCLUSIONS

We performed a closure study in the broadband thermal range and in the atmospheric window using the RTM libRadtran (with absorption calculations based on ARTS and LOWTRAN), MODTRAN and measurements in the corresponding wavelength ranges. Results for the atmospheric window showed best agreement between the line-by-line tool ARTS and the measurements within  $1 \text{ Wm}^{-2}$ . Also the moderate resolution model MODTRAN was within the measurement uncertainties of about  $2 \text{ Wm}^{-2}$  and  $1 \text{ Wm}^{-2}$  for the broadband range and atmospheric window respectively. Only the results of the lower resolved LOWTRAN were significantly outside of the uncertainties. Furthermore we showed by comparing measurements and MODTRAN calculations performed with normalized standard atmospheres scaled to the total IWV content that in the atmospheric window, LDR is mainly driven by the total water content: the mean result was almost as close to the uncertainty range ( $1 \text{ Wm}^{-2}$ ) as with profiles obtained from radiosondes. As a consequence, LDR can be simulated in the atmospheric window by applying scaled standard profiles and an adequate resolved RTM. However, this is not valid for the broadband range where LDR not only depends on the water vapor content but also on temperature. Hence, an accurate temperature profile is additionally required to model LDR precisely in the broadband range. We showed that pyrgeometer measurements in the atmospheric window in combination with RTM will be a promising tool to analyse the variability of LDR. Finally, the investigation revealed that pyrgeometers, sensitive only in the atmospheric window, are an attractive addition to support explicit validation of RTM in the regime of not saturated water vapor spectra in the atmospheric window.

## ACKNOWLEDGMENTS

We thank MeteoSwiss for providing us with LDR, pressure, temperature, humidity and radiosonde data and the Institute of Applied Physics of the University Bern for IWV data.

## REFERENCES

1. B. Albrecht, M. Poellot and S. K. Cox, "Pyrgeometer measurements from aircraft", *Rev. Sci Instrum.* **45**, 33-38 (1974).
2. R. Philipona, E. G. Dutton, T. Stoffel, J. Michalsky, I. Reda, A. Stifter, P. Wendling, N. Wood, S. A. Clough, E. J. Mlawer, G. Anderson, H. E. Revercomb, and T. R. Shippert, "Atmospheric longwave irradiance uncertainty: pyrgeometers compared to an absolute sky-scanning radiometer, atmospheric emitted radiance interferometer, and radiative transfer model calculations," *J. Geophys. Res.* **106**, 28129–28141, (2001).
3. J. Gröbner and A. Los, "Laboratory calibration of pyrgeometers with known spectral responsivities", *Appl. Opt.* **46**, 7419-7425 (2007).
4. P. Jeannet (private communication).
5. J. Morland, B. Deuber, D. G. Feist, L. Martin, S. Nyeki, N. Kämpfer, C. Mätzler, P. Jeannet and L. Vuilleumier, "The STARTWAVE atmospheric water database", *Atmos. Chem. Phys.* **6**, 2039-2056 (2006).
6. B. Dürr, R. Philipona, F. Schubiger and A. Ohmura, "Comparison of modeled and observed cloud-free longwave downward radiation over the Alps", *Meteorol. Zeitschr.* **14**, 47-55 (2004).
7. B. Dürr and R. Philipona, "Automatic cloud amount detection by surface longwave downward radiation measurements", *J. Geophys. Res.* **109**, doi:10.1029/2003JD004182 (2004).
8. B. Mayer and A. Killing, "Technical note: The libRadtran software package for radiative transfer calculations-description and examples of use", *Atmos. Chem. Phys.* **4**, 1255-1263 (2005).
9. A. Berk, G.P. Anderson, P.K. Acharya, J.H. Chetwynd, L.S. Bernstein, E.P. Shettle, M.W. Matthew and S.M. Adler-Golden, "MODTRAN4 User's Manual", Air Force Research Laboratory Report (1999).
10. S.A. Buehler, P. Eriksson, T. Kuhn, A. von Engeln and C. Verdes, "ARTS, the Atmospheric Radiative Transfer Simulator", *J. Quant. Spectrosc. Radiat. Transfer*, **91(1)**, 65-93 (2005).
11. J.H. Pierluissi and G.-S. Peng, 'New molecular transmission band models for LOWTRAN', *Optical Engineering*, **24**, 541-547 (1985).
12. P. Ricchiazzi, S. Yang, C. Gautier, and D. Sowle, 'SBDART: A research and teaching software tool for plane-parallel radiative transfer in the Earth's atmosphere', *Bull. Am. Met. Soc.* **79**, 2101-2114 (1998).